ACS APPLIED MATERIALS & INTERFACES

Research Article

www.acsami.org

Systematic Investigations on the Roles of the Electron Acceptor and Neighboring Ethynylene Moiety in Porphyrins for Dye-Sensitized Solar Cells

Tiantian Wei,[†] Xi Sun,[†] Xin Li,[*,‡] Hans Ågren,[‡] and Yongshu Xie[*,†]

[†]Key Laboratory for Advanced Materials and Institute of Fine Chemicals, East China University of Science & Technology, Shanghai 200237, P. R. China

[‡]Division of Theoretical Chemistry and Biology, School of Biotechnology, KTH Royal Institute of Technology, SE-10691 Stockholm, Sweden

Supporting Information

ABSTRACT: Cyanoacrylic and carboxyl groups have been developed as the most extensively used electron acceptor and anchoring group for the design of sensitizers for dye-sensitized solar cells. In terms of the photoelectric conversion efficiency, each of them has been demonstrated to be superior to the other one in certain cases. Herein, to further understand the effect of these two groups on cell efficiencies, a series of porphyrin sensitizers were designed and synthesized, with the acceptors systematically varied, and the effect of the neighboring ethynylene unit was also investigated. Compared with the sensitizer **XW5** which contains a carboxyphenyl anchoring moiety directly linked to the meso-position of the porphyrin framework, the separate introduction of a strongly electron-withdrawing cyanoacrylic acid as the anchoring group or the insertion of an ethynylene unit can achieve broadened light absorption and IPCE response, resulting in higher J_{sc} and higher efficiency. Thus, compared with the efficiency of 4.77% for **XW5**, dyes **XW1** and **XW6** exhibit higher efficiencies of 7.09% and 5.92%, respectively. Simultaneous introduction of the cyanoacrylic acid and the ethynylene units into **XW7** can further broaden light absorption and thus further improve the J_{sc}. However, **XW7** exhibits the lowest V_{oc} value, which is not only related to the floppy structure of the cyanoacrylic group but also related to the aggravated dye aggregation effect due to the extended framework. As a result, **XW7** exhibits a relatively low efficiency of 5.75%. These results indicate that the combination of the ethynylene and cyanoacrylic groups is an unsuccessful approach. To address this problem, a cyano substituent was introduced to **XW8** at the ortho position of the carboxyl group in the carboxyphenyl acceptor. Thus, **XW8** exhibits the highest efficiency of 7.59% among these dyes. Further cosensitization of **XW8** with **XS3** dramatically improved the efficiency to 9.31%.

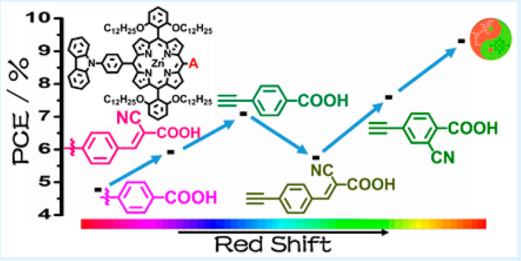

KEYWORDS: *dye-sensitized solar cells, porphyrin, anchoring groups, π-linkers, cyano group*

INTRODUCTION

With increasing demand for clean and renewable energy, various approaches for solar energy conversion have been developed over the past decades. Among them, dye-sensitized solar cells (DSSCs) have been demonstrated to have the advantages of relatively low cost, high efficiency, and easy fabrication. Since first reported by Grätzel and co-workers in 1991,[1] various sensitizers with electron donor−π bridge−electron acceptor (D−π−A) frameworks have been developed for fabricating efficient DSSCs.[2−14]

Porphyrins and porphyrin analogues have been widely used in the field of functional materials because of their strong absorption, excellent electronic properties, and easy structural modification.[15−22] Especially, D−π−A type zinc porphyrin sensitizers have been used as efficient sensitizers in the past decade.[23−30] Up to date, the highest photoelectric conversion efficiency (PCE) record of ∼13% was achieved by a zinc porphyrin dye SM315.[31] Photovoltaic behavior of a zinc porphyrin sensitizer is highly dependent on the donor and the acceptor.[32−38] As an electron donor, carbazole has been widely used in developing sensitizers.[36−39] In this respect, we have designed carbazole-based sensitizers **XW1**−**XW4**, achieving the high efficiency of 10.45% through a combined approach of molecular structure optimization and cosensitization.[37] On the other hand, the carboxylic acid group has been extensively used as the electron acceptor and the anchoring group.[10] To further enhance the electron-withdrawing character, red-shift the absorption bands, and improve the electron injection ability, the cyanoacrylic group was used as the electron acceptor in a number of sensitizers.[39−54] In spite of these successful examples, the floppy structure of the cyanoacrylic group was also observed to decrease the cell efficiencies in some cases.[33,34,40,41] Thus, correlation between the electron acceptor and the cell efficiency still remains rather elusive. On the other

Received: July 21, 2015
Accepted: September 10, 2015
Published: September 10, 2015

DOI: 10.1021/acsami.5b06610
ACS Appl. Mater. Interfaces 2015, 7, 21956−21965

Chart 1. Chemical Structures of the Porphyrin Dyes and the Cosensitizer XS3[a]

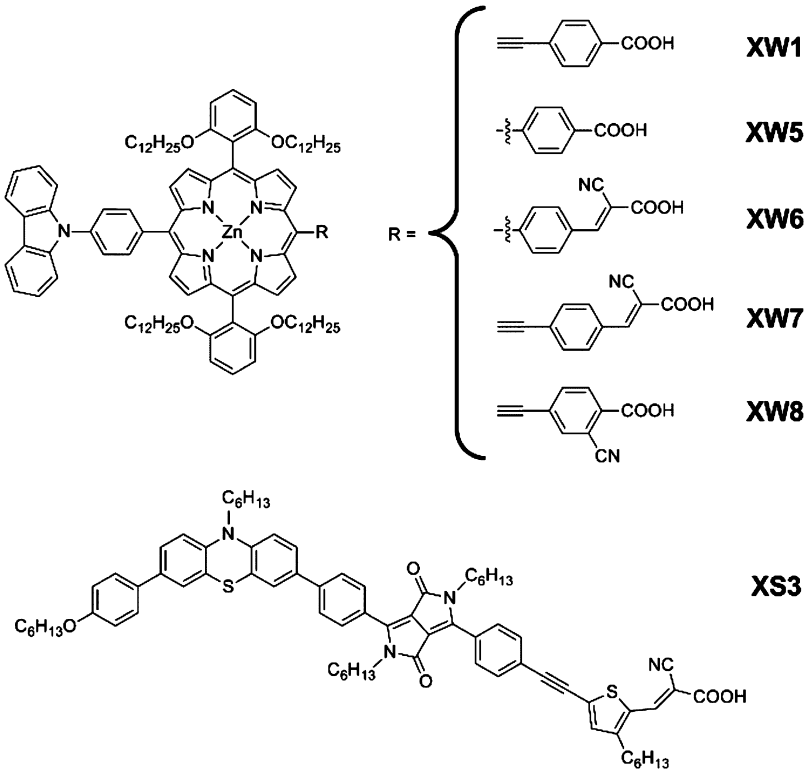

[a]**XW1** and **XS3** have been reported in our previous papers.[37,46]

hand, the combination of an ethynylene unit with the acceptor is also an effective approach for extending the absorption wavelength range,[40−42] but this approach further complicates the acceptor−efficiency correlation.[40,41] Hence, further work is highly desired with the purpose to understand the correlation and thus provide further insights into developing efficient sensitizers.

As mentioned above, it has been demonstrated that cosensitization of two dyes with complementary absorption spectra is also an effective approach for enhancing the light harvesting efficiency and thus achieve an PCE higher than both of the individual dyes.[10,37,46]

On the basis of the aforementioned background and our previous work on **XW1**−**XW4**, we herein report the design and synthesis of **XW1** derivatives, **XW5**−**XW8** (Chart 1). The effect of the acceptor and the ethynylene unit on the cell efficiency was systematically investigated. Compared with **XW5**, separate incorporation of the cyanoacrylic and acetylene groups in **XW6** and **XW1** can efficiently red-shift light response of the dyes, which is favorable for enhancing the sunlight harvesting efficiency and the cell efficiency. However, concurrence of these two groups in **XW7** caused enhanced charge recombination rate and drastically decreased V_{oc}, thus resulting in a relatively low PCE of 5.75%. In contrast, in **XW8**, the cyano group was introduced to the ortho-position of the carboxyl group in the carboxyphenyl acceptor, and thus the PCE was improved to 7.59%. Furthermore, a high PCE of 9.31% was achieved through cosensitization of **XW8** and **XS3**. These results provide further insights into optimizing the porphyrin sensitizer structures as well as the cosensitization approach for developing efficient DSSCs.

RESULTS AND DISCUSSION

Syntheses and Characterization. As depicted in Scheme 1, intermediate **5**[37] was used to react with **1**−**4** through Suzuki or Sonogashira coupling reactions to afford the intermediates **1s**−**3s** and the target molecule **XW8**. Finally, the target sensitizers were obtained through hydrolysis or Knoevenagel condensation reactions. Consequently, dyes **XW5**−**XW8** were successfully synthesized in acceptable yields and fully characterized with NMR and HRMS (Figures S1−S11).

Optical Properties. The new porphyrin dyes **XW5**−**XW8** as well as **XW1** exhibited typical metalloporphyrin features of an intense Soret band and moderate Q bands. UV−vis absorption spectra of all the five dyes are presented in Figure 1. The peak positions and molar absorption coefficients obtained in THF are listed in Table 1.

It is obvious that the acetylene group can dramatically red shift the absorption peaks. Take the low-energy peaks, for example, **XW1** and **XW7**, which exhibit 28 and 32 nm red shift as compared to **XW5** and **XW6**, respectively. In contrast, the cyanoacrylic group only induces a slight red shift as compared with the carboxyphenyl group. Thus, **XW6** and **XW7** exhibit 5 and 9 nm red shift as compared to **XW5** and **XW1**, respectively. On the other hand, **XW8** contains a cyano group on the carboxyphenyl moiety at the ortho-position relative to −COOH, and an ethynylene unit was incorporated between the carboxy-phenyl moiety and the porphyrin framework. Because of the extended framework and the strong electron-withdrawing CN group, its lowest-energy peak is centered at 665 nm, which is red-shifted by 29−66 nm, as compared with the other four dyes. From the absorption spectra, it can be concluded that insertion of an acetylene unit and/or introducing a stronger electron-withdrawing moiety as the

DOI: 10.1021/acsami.5b06610
ACS Appl. Mater. Interfaces 2015, 7, 21956−21965

Scheme 1. Synthetic Route for XW5−XW8*

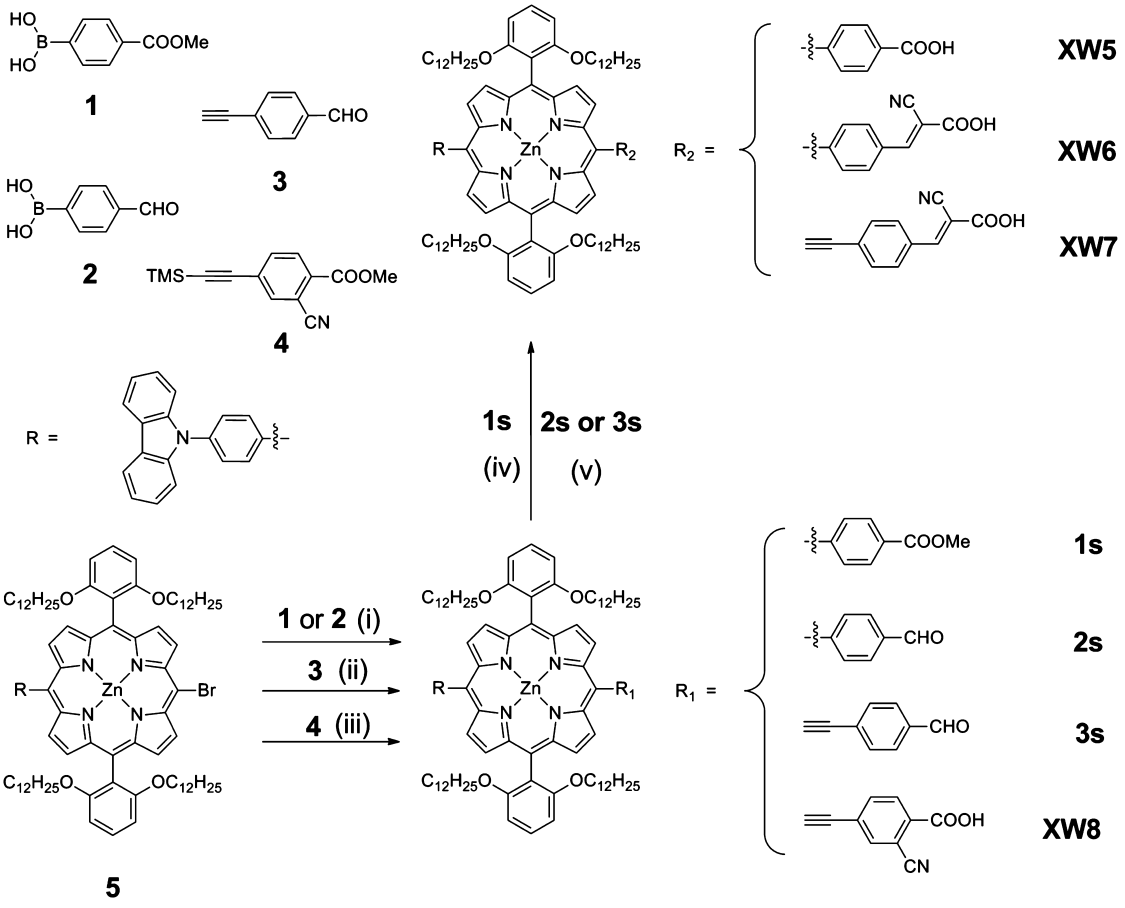

*Reaction conditions: (i) $Pd(PPh_3)_4$, 2 M Na_2CO_3, PhMe, EtOH; (ii) $Pd(PPh_3)_4$, CuI, Et_3N, THF; (iii) $Pd(PPh_3)_4$, CuI, K_2CO_3, piperidine, THF, MeOH; (iv) $LiOH{\cdot}H_2O$, THF, H_2O; (v) cyanoacetic acid, piperidine, THF.

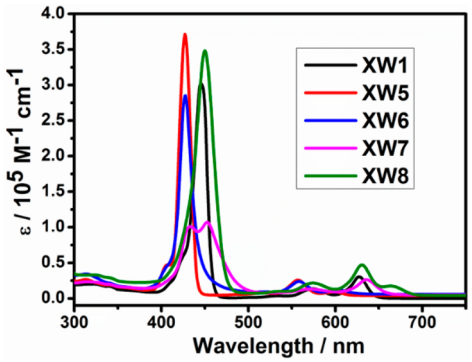

Figure 1. UV−vis adsorption spectra of the dyes in THF solution.

Table 1. Absorption and Emission Data for the Dyes in THF

dyes	absorption λ_{max} [nm] (ε [10^3 M^{-1} cm^{-1}])[a]	emission λ_{max} [nm][a]
XW5	427 (370), 557 (26.0), 599(9.7)	609, 657
XW6	428 (285), 558 (23.8), 604(11.2)	617
XW7	432 (101), 453 (108), 573 (13.1), 636 (26.5)	648
XW8	450 (349), 574 (21.7), 631(47.0) 665 (17.4)	641
XW1[b]	446 (302), 574 (13.6), 627 (30.4)	638

[a]The absorption and emission data were measured in THF. Excitation wavelengths/nm: 446 nm (**XW1**), 427 nm (**XW5**), 427 nm (**XW6**), 453 nm (**XW7**), 450 nm (**XW8**). [b]The data were reported in our previous work.[37]

electron acceptor is favorable for extending the absorption and improving the light harvesting ability. Especially, **XW8** demonstrates the most extensive absorption range among these dyes, which is favorable for harvesting the sunlight.

The photovaoltaic behavior is directly related to the absorption spectra of the dyes adsorbed on the TiO_2 film. Upon adsorption on TiO_2, all the dyes showed broadened Soret and Q bands, which is favorable for absorbing the sunlight (Figure S12).

Theoretical Calculations. Suitable spatial distributions of the frontier orbitals are essential for DSSCs. Toward a better understanding of the frontier molecular orbitals of the sensitizers, density functional theory (DFT) calculations were performed, and the corresponding contour plots are illustrated in Figure 2. For all the dyes, the HOMO orbitals are mainly distributed over the donor and the porphyrin framework, while the LUMO orbitals are predominantly distributed over the porphyrin framework and the acceptor, which can result in redistribution of the electron from the HOMO to the LUMO and thus enabling the electron transfer from the donor to the anchoring group and successive electron injection from the LUMO to the conduction band of TiO_2. In the optimized molecular structures, the dihedral angles between the porphyrin cores and the anchoring phenylene groups are quite different. Without an ethynylene linker, the molecules are highly distorted, with large dihedral angles of 66.0° and 62.7° for

DOI: 10.1021/acsami.5b06610
ACS Appl. Mater. Interfaces 2015, 7, 21956−21965

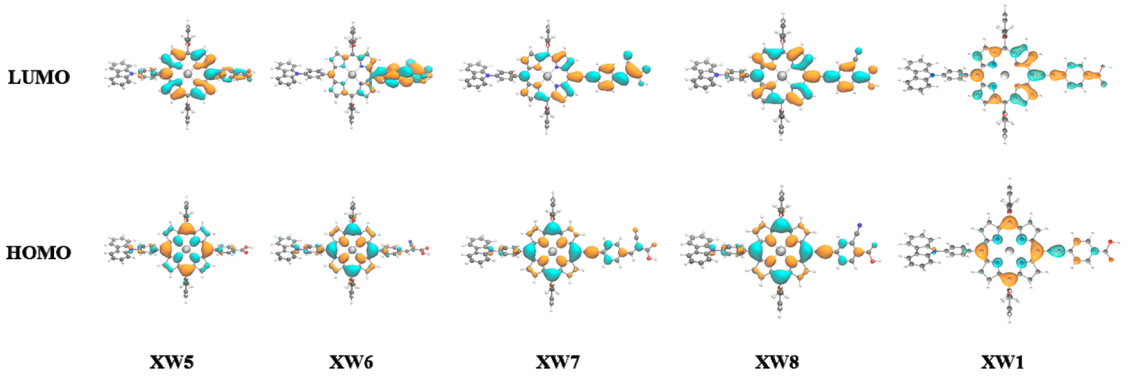

Figure 2. Frontier molecular orbital profiles of the dyes calculated by DFT.

XW5 and **XW6**, respectively. In contrast, **XW7** and **XW8**, as well as **XW1**, exhibit very small angles of nearly 0°, indicating that the presence of the ethynylene unit can significantly improve the planarity and π-conjugation, which is consistent with the observation of red-shifted absorption peaks, as compared with **XW5** and **XW6**. It is noteworthy that the LUMOs of **XW6**–**XW8** are much more delocalized than that of **XW5**, indicative of the strong ICT character caused by the presence of the electron-withdrawing CN group. Time-dependent DFT calculations show that both the maximum absorption wavelengths and the corresponding oscillator strengths follow the order **XW7** > **XW8** > **XW1** > **XW6** > **XW5** (Table S1, Figures S13–14). It is clear that **XW5** is not an ideal sensitizer due to its highly localized excitation at the porphyrin core. Although the HOMO and LUMO of **XW6** indicate large charge-transfer excitation, the lowest excited state of **XW6** contains mixed electronic transitions from several frontier molecular orbitals, such that the maximum absorption wavelength is shorter than those of **XW7** and **XW8**. The computational results are in accordance with the experimentally measured short-circuit current and photovoltaic efficiency except for **XW7**, and **XW8** exhibits the best performance among all the investigated sensitizers (*vide infra*).

Electrochemical Properties. Electrochemical properties of the dyes could illustrate the possibility of electron transfer processes. Thus, cyclic voltammetry measurements were performed (Table 2 and Figures S15–S16).

HOMO levels of **XW5**–**XW8** are 0.70, 0.79, 0.84, and 0.87 V, respectively, and the LUMO levels are estimated to be −1.51, −1.32, −1.13, and −1.13 V, respectively. Obviously, the LUMO levels of all the dyes lie well above the conduction band of TiO_2 (−0.5 V vs NHE). Meanwhile, the HOMO levels lie below the iodide/triiodide redox potential (0.4 V vs NHE), indicating that both the electron injection and dye regeneration processes are feasible.[55] **XW7** and **XW8**, as well as **XW1**, exhibit narrower HOMO–LUMO energy gaps and relatively positive LUMO orbitals relative to those for **XW5** and **XW6**, resulting from the presence of an additional ethynylene bridge, which is also consistent with the red shift of the absorption bands.

Table 2. Absorption and Emission Data for the Dyes in THF

	HOMO [V][a]	E_{0-0} [eV][b]	LUMO [V][c]
XW5	0.70	2.21	−1.51
XW6	0.79	2.11	−1.32
XW7	0.84	1.97	−1.13
XW8	0.87	2.00	−1.13
XW1	0.87	1.96	−1.09

[a]HOMO levels were measured in acetonitrile with 0.1 M tetra-*n*-butylammonium hexafluorophosphate ($TBAPF_6$) as electrolyte (working electrode: FTO/TiO_2/dye; reference electrode: SCE; calibrated with ferrocene/ferrocenium (Fc/Fc^+) as an external reference. Counter electrode: Pt. [b]E_{0-0} was estimated from the intersection wavelengths of the normalized UV–visible absorption and the fluorescence spectra. [c]The LUMO was calculated using the equation LUMO = HOMO − E_{0-0}.

Photovoltaic Performance of DSSCs. On the basis of the above-mentioned results, the dyes were used for fabrication of DSSCs, and the corresponding photovoltaic parameters are summarized in Table 3. The photocurrent–voltage curves and the incident photon-to-current conversion efficiency (IPCE) action spectra are shown in Figure 3.

Table 3. Summary of DSSC Performance Parameters for Dyes and Cosensitization

dyes	J_{sc} [mA cm^{-2}]	V_{oc} [mV]	FF	PCE [%]
XW1	14.36	713	0.69	7.09
XW5	10.65	648	0.69	4.77
XW6	12.19	689	0.70	5.92
XW7	13.10	610	0.72	5.75
XW8	15.72	700	0.69	7.59
XS3	15.69	739	0.69	7.94
XW1+XS3[a]	17.17	723	0.70	8.75
XW8+XS3[a]	18.23	705	0.73	9.31
XW1[b]	14.99	716	0.66	7.13
XS3[b]	15.73	748	0.68	8.02

[a]The cosensitization was performed through an optimized stepwise approach: the TiO_2 electrode was first dipped in 0.2 mM of the porphyrin dye in toluene/ethanol (v/v, 1/4) for 10 h, rinsed with ethanol, and then immersed in a 0.3 mM solution of **XS3** in chloroform/ethanol (v/v, 3/7) for 1 h. [b]The data were reported in our previous studies.[37,46]

The obtained power conversion efficiencies (PCEs) lie in the range of 4.77%–7.59% in the order of **XW5** < **XW7** < **XW6** < **XW1** < **XW8**, indicative of the significant influences of the ethynylene unit and the anchoring groups on the photovoltaic performances of the DSSCs. As observed from Figure 3(a), the bandwidths of the IPCE spectra were observed to be increased in the order of **XW5** < **XW6** < **XW1** < **XW7** < **XW8**, which is consistent with the corresponding absorption spectra. However, the short-circuit current density (J_{sc}) values exhibit a slightly different order of **XW5** < **XW6** < **XW7** < **XW1** < **XW8**, where the J_{sc} for **XW7** is lower than that of **XW1**. This observation

DOI: 10.1021/acsami.5b06610
ACS Appl. Mater. Interfaces 2015, 7, 21956–21965

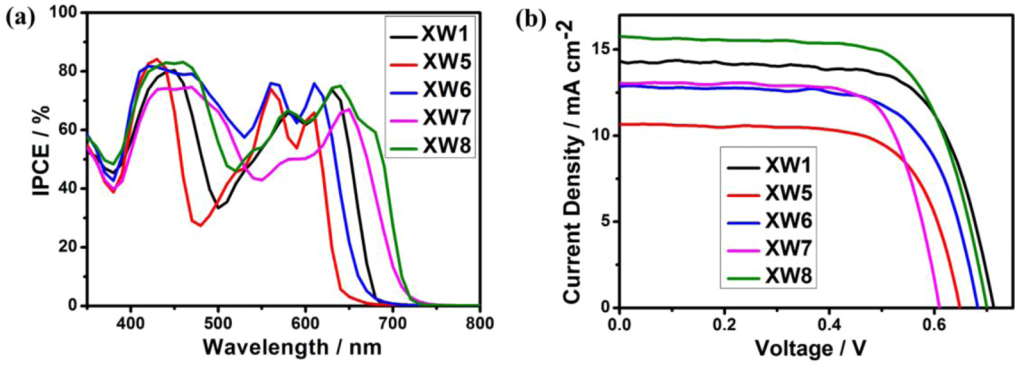

Figure 3. (a) IPCE action spectra for the DSSCs based on **XW5**–**XW8** and **XW1**. (b) J–V characteristics of the DSSCs.

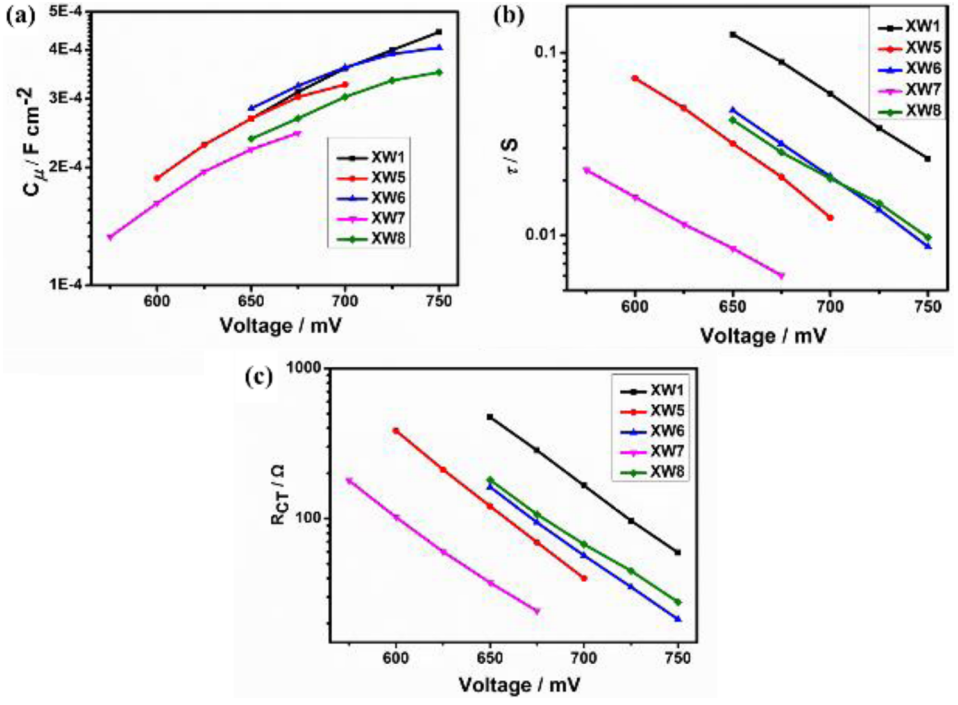

Figure 4. Chemical capacitance C_μ (a), electron lifetime τ (b), and interfacial charge transfer resistance R_{CT} (c) of the cells based on **XW5**–**XW8** and **XW1** as a function of bias voltage.

might be ascribed to the lower IPCE values of **XW7** than those of **XW1** in large wavelength ranges of 300–460 nm and 530–640 nm.

Open-circuit voltage (V_{oc}) is also an essential parameter for DSSCs. The obtained V_{oc} for **XW7** is 610 mV, which is dramatically lower than that of 713 mV for **XW1**. This observation may be ascribed to the floppy structure associated with the cyanoacrylic acid group.[33,34,40,41] Actually, among all these dyes, **XW7** exhibited the lowest V_{oc} value, which is not only related to the floppy structure of the cyanoacrylic group but also related to the aggravated dye aggregation effect due to the extended framework of coexisting ethynylene and cyanoacrylic moieties.[40,41,56] These results indicate that the combination of the ethynylene and cyanoacrylic groups turns out to be an unsuccessful approach. In contrast, in **XW8**, a cyano substituent was introduced to the ortho-position of the carboxyl group in the carboxyphenyl acceptor. Compared with **XW7**, **XW8** exhibited much higher V_{oc} of 700 mV and a higher PCE of 7.59%.

Contrary to the tendency observed for **XW7** and **XW1**, the cyanoacrylic moiety containing dye **XW6** exhibited a higher V_{oc} than the corresponding carboxyphenyl containing dye **XW5**, indicating that the relative performance of the carboxyphenyl and the cyanoacrylic anchoring groups may be dependent on the presence of the ethynylene moiety; i.e., with a concurrent ethynylene moiety, the carboxyphenyl moiety tends to afford a higher V_{oc}, and the cyanoacrylic moiety tends to provide a higher V_{oc} in the absence of the ethynylene moiety. To further understand the discrepant tendency, we continued to check the electrochemical impedance spectroscopy.

Electrochemical Impedance Spectroscopy. As we know, the V_{oc} of a DSSC is dependent on the electron quasi-Fermi-level (E_f) in TiO_2, which can be inferred from the chemical capacitance (C_μ) values. On the other hand, V_{oc} is also related to the electron lifetime. Thus, electrochemical impedance spectroscopy (EIS) measurements were carried out at different potential bias. The chemical capacitance (C_μ), the interfacial charge transfer resistance (R_{CT}), and the electron lifetime (τ) were obtained through fitting the EIS spectra.[58]

DOI: 10.1021/acsami.5b06610
ACS Appl. Mater. Interfaces 2015, 7, 21956–21965

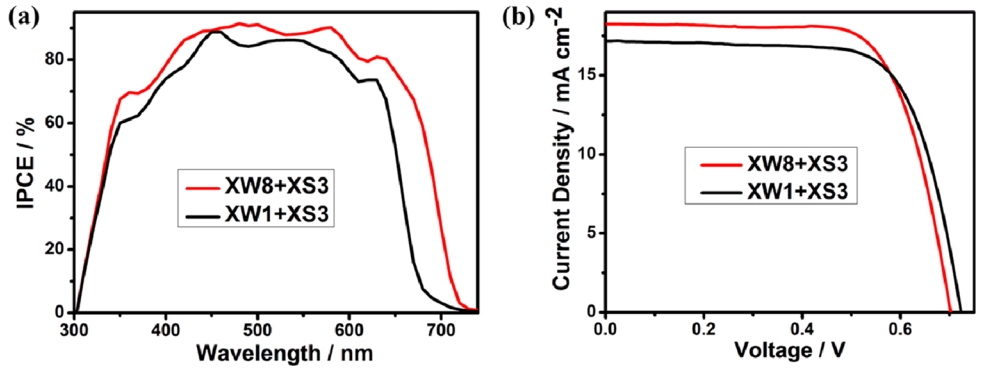

Figure 5. (a) IPCE action spectra and (b) the $J-V$ characteristics of the cosensitized DSSCs.

The plots of C_μ values shown in Figure 4 demonstrate that the positions of the conduction band edge of sensitized TiO_2 are dependent on the acceptors of the dyes. **XW7** and **XW8** showed smaller capacitance data than the other dyes, indicating a negative shift of the conduction band edge.[31,57,58] As shown in Figure 4, at a given voltage bias, the fitted R_{CT} and τ lie in the order of **XW7** < **XW5** < **XW6** < **XW8** < **XW1**, suggesting the same order of decreasing charge recombination rate and increasing electron lifetime.[58] Among these dyes, the relatively low C_μ values observed for **XW7** tend to improve the V_{oc}, and the small R_{CT} and τ values tend to decrease the V_{oc}. Coexistence of these conflicting effects finally affords a lowest V_{oc} value for **XW7** among all these dyes, and the order for R_{CT} and τ agrees well with that of the V_{oc} values, indicating that the V_{oc} is mainly dependent on the charge recombination process, instead of the electron quasi-Fermi-level in TiO_2.

Photostability. Photostability is essential for real applications of DSSCs. In order to investigate the effects of different anchoring groups on the photostability, the dyes were adsorbed on the TiO_2 photoanode films and subsequently irradiated under standard one-sun illumination for 0, 5, 15, and 30 min, respectively. The recorded UV–vis spectra are shown in Figure S17. All the dyes show acceptable to excellent photostability. Notably, **XW6** demonstrates much better photostability than the other dyes, which may be related to the presence of the cyanoacrylic anchoring group and absence of the ethynylene unit.

Cosensitization. As mentioned above, **XW8** and **XW1** exhibit the higher efficiencies among all the dyes. However, it is also obvious that its IPCE curve exhibits two absorption valleys around 520 and 380 nm (Figure 3). Fortunately, our previously reported dye **XS3** (Chart 1)[46] has two absorption peaks exactly in these two wavelength ranges. Hence, it can be anticipated that cosensitization of these porphyrin dyes with **XS3** may afford higher efficiencies. Therefore, we fabricated DSSCs through cosensitization of **XW8** and **XW1** with **XS3** and checked the photovoltaic behavior (Table 3, Figure 5, and Figure S18). As can be seen from the IPCE curve (Figure 5a), both absorption valleys of **XW8** and **XW1** are well filled up. Thus, for **XW8**, the IPCE values are higher than 70% in a large wavelength range of 360–670 nm. As a result, the J_{sc} value of the cosensitized DSSC is dramatically improved to 18.23 mA cm^{-2}, and the efficiency is enhanced to 9.31%. Similarly, a PCE of 8.75% was achieved for the cosensitization of **XW1** and **XS3**.

CONCLUSIONS

In summary, porphyrin sensitizers containing a carbazole electron donor were designed, synthesized, fully characterized, and used for fabricating dye-sensitized solar cells. In these dyes, the systematically varied acceptors and the neighboring ethynylene units exhibit a dramatic effect on the photovoltaic behavior. Compared with sensitizer **XW5** which contains a carboxyphenyl anchoring moiety directly linked to the meso-position of the porphyrin framework, the separate introduction of a strongly electron-withdrawing cyanoacrylic acid as the anchoring group or the insertion of an ethynylene unit can achieve broadened light absorption and IPCE response, resulting in higher J_{sc} and higher photoelectric conversion efficiency. Thus, compared with the efficiency of 4.77% for **XW5**, dyes **XW1** and **XW6** exhibit higher efficiencies of 7.09% and 5.92%, respectively. Simultaneous introduction of the cyanoacrylic acid and the ethynylene units into **XW7** can further broaden light absorption and thus improve the J_{sc} from that of 12.19 mA cm^{-2} for **XW6** to 13.10 mA cm^{-2}. However, **XW7** exhibits the lowest V_{oc} value, which is not only related to the floppy structure of the cyanoacrylic group but also related to the aggravated dye aggregation effect due to the extended framework. As a result, **XW7** exhibits a relatively low efficiency of 5.75%. To avoid the drawbacks of the cyanoacrylic group, a cyano substituent was introduced to **XW8** at the ortho-position of the carboxyl group in the carboxyphenyl acceptor. Thus, **XW8** exhibits a highest J_{sc} of 15.72 mA cm^{-2}, a high V_{oc} of 700 mV, and a highest PCE of 7.59% among all these dyes. Electrochemical impedance spectroscopy measurements revealed that the V_{oc} values for these dyes are mainly dependent on the charge recombination processes, instead of the electron quasi-Fermi-levels in TiO_2. Furthermore, upon cosensitization of **XW8** with **XS3**, absorption valleys of **XW8** are well filled up. As a result, the J_{sc} value and the efficiency were dramatically improved to 18.23 mA cm^{-2} and 9.31%, respectively.

These results provide further insight into optimizing the porphyrin sensitizer structures by considering the combined effect of the acceptor and the neighboring ethynylene unit, and cosensitization has been demonstrated to be effective for further improving the cell efficiencies. Investigations on developing novel porphyrin sensitizers for further efficiency–structure correlations are underway in our group in the following respects: excluding the ethynylene unit from **XW8** and varying the substitution positions of the carboxyl and the cyano groups.[59]

EXPERIMENTAL SECTION

Reagents and Equipment. All chemicals and solvents were purchased from commercial sources and used without further purification unless otherwise noted. The TiO_2 paste and the transparent FTO conducting glass (fluorine-doped SnO_2, transmission

DOI: 10.1021/acsami.5b06610
ACS Appl. Mater. Interfaces 2015, 7, 21956–21965

>90% in the visible range, sheet resistance 15Ω/square) were purchased from Geao Science and Educational Co. Ltd. Besides, the FTO glass was washed with a detergent solution, deionized water, ethanol, and acetone successively under ultrasonication for 20 min before use. ^{1}H NMR and ^{13}C NMR spectra were obtained using a Bruker AM 400 spectrometer. HRMS measurements were performed using a Waters LCT Premier XE spectrometer. UV−vis absorption spectra in solution and adsorbed on TiO_2 films were recorded on a Varian Cary 100 spectrophotometer, and fluorescence spectra were recorded on a Varian Cray Eclipse fluorescence spectrophotometer. FT-IR spectra were recorded in the region of 400−4000 cm^{-1} on a Thermo Electron Avatar 380 FT-IR instrument (KBr Discs).

Synthesis and Characterization of the Dyes. The main synthetic pathways were presented in Scheme 1. All the four new dyes were synthesized from the starting compound of porphyrin **5**, which was prepared as reported ealier.[37] **1** and **2** were purchased from commercial sources and used as received. **3** and **4** were synthesized according to the reported procedures.[34,60]

1s: A mixture of porphyrin **5** (100 mg, 0.063 mmol), **1** (58 mg, 0.32 mmol), $Pd(PPh_3)_4$ (9 mg, 0.008 mmol), Na_2CO_3 (67 mg, 0.63 mmol) in PhMe (30 mL), and EtOH (6 mL) was refluxed for 5 h under nitrogen. Then, the solvent was removed in vacuo. The residue was dissolved in CH_2Cl_2 and washed with water, dried over anhydrous sodium sulfate, and evaporated to afford the crude product, which was purified by chromatography on silica gel columns. Recrystallization from CH_2Cl_2/CH_3OH gave the target compound (92 mg, yield 89%). ^{1}H NMR ($CDCl_3$, 400 MHz, ppm): 0.37−0.52 (m, 24H), 0.62−0.69 (m, 8H), 0.76−0.81 (m, 20H), 0.87−1.16 (m, 40H), 3.83 (t, J = 6.4 Hz, 8H), 4.01 (s, 3H), 7.00 (d, J = 8.4 Hz, 4H, phenyl), 7.40 (t, J = 6.8 Hz, 2H, phenyl), 7.58 (t, J = 7.2 Hz, 2H, phenyl), 7.69 (t, J = 8.4 Hz, 2H, phenyl), 7.83 (d, J = 8.4 Hz, 2H, phenyl), 7.94 (d, J = 8.4 Hz, 2H, phenyl), 8.26 (t, J = 7.6 Hz, 2H, phenyl), 8.31 (d, J = 8.0 Hz, 2H, phenyl), 8.41 (d, J = 8.0 Hz, 2H, phenyl), 8.45 (d, J = 8.0 Hz, 2H, phenyl), 8.80 (d, J = 4.4 Hz, 2H, pyrrolic), 8.91 (d, J = 4.8 Hz, 2H, pyrrolic), 8.96 (d, J = 4.4 Hz, 2H, pyrrolic), 9.00 (d, J = 4.8 Hz, 2H, pyrrolic). ^{13}C NMR ($CDCl_3$, 100 MHz,): δ 13.02, 21.56, 24.13, 27.53, 27.65, 28.01, 28.16, 30.76, 48.88, 51.26, 52.37, 67.55, 104.20, 109.00, 102.49, 117.09, 119.41, 123.66, 127.79, 130.23, 133.60, 140.01, 147.59, 149.68, 158.99, 166.53. MALDI-TOF-MS: calcd for $C_{106}H_{133}N_5O_6Zn$, 1635.95; found, 1636.33.

2s: It was prepared according to the same procedure as that for **1s**, except that **2** (48 mg, 0.32 mmol) was used instead of **1**. ^{1}H NMR ($CDCl_3$, 400 MHz, ppm): 0.35−0.43 (m, 8H), 0.49−0.56 (m, 16H), 0.62−0.69 (m, 10H), 0.76−0.81 (m, 20H), 0.87−1.04 (m, 32H), 1.12−1.16 (m, 6H), 3.84 (t, J = 6.4 Hz, 8H), 7. 00 (t, J = 8.4 Hz, 4H, phenyl), 7.40 (t, J = 7.6 Hz, 2H, phenyl), 7.58 (t, J = 6.8 Hz, 2H, phenyl), 7.70 (t, J = 8.4 Hz, 2H, phenyl), 7.83 (t, J = 8.4 Hz, 2H, phenyl), 7.94 (d, J = 8.4 Hz, 2H, phenyl), 8.25 (t, J = 4.0 Hz, 2H, phenyl), 8.27 (d, J = 4.0 Hz, 2H, phenyl), 8.41 (d, J = 8.0 Hz, 2H, phenyl), 8.45 (d, J = 8.0 Hz, 2H, phenyl), 8.79 (d, J = 4.8 Hz, 2H, pyrrolic), 8.93 (d, J = 4.4 Hz, 2H, pyrrolic), 8.96 (d, J = 4.8 Hz, 2H, pyrrolic), 9.00 (d, J = 4.8 Hz, 2H, pyrrolic), 10.38 (s, 1H). ^{13}C NMR ($CDCl_3$, 100 MHz): δ 14.10, 22.63, 25.20, 28.60, 28.72, 29.08, 29.24, 29.33, 29.46, 31.83, 68.61, 105.25, 110.06, 117.69, 120.49, 124.74, 129.77, 131.50, 135.29, 141.06, 148.97, 150.84, 160.04, 192.62. MALDI-TOF-MS: calcd for $C_{105}H_{131}N_5O_5Zn$, 1605.94; found, 1606.47.

3s: A mixture of the porphyrin **5** (100 mg, 0.063 mmol), **3** (42 mg, 0.32 mmol), $Pd(PPh_3)_4$ (11 mg, 0.01 mmol), CuI (2 mg, 0.01 mmol) in THF (30 mL), and Et_3N (3 mL) was refluxed for 5 h under nitrogen. Then, the solvent was removed in vacuo. The residue was purified by column chromatography on silica gel columns. Yield: 44 mg, 43%. ^{1}H NMR ($CDCl_3$, 400 MHz, ppm): 0.40−0.45 (m, 8H), 0.49−0.57 (m, 15H), 0.61−0.69 (m, 10H), 0.77−0.82 (m, 25H), 0.86−0.92 (m, 10H), 0.96−1.03 (m, 16H), 1.09−1.16 (m, 8H), 3.87 (t, J = 6.4 Hz, 8H), 7.02 (d, J = 8.4 Hz, 4H, phenyl), 7.40 (t, J = 7.2 Hz, 4H, phenyl), 7.57 (t, J = 8.0 Hz, 2H, phenyl), 7.72 (t, J = 8.4 Hz, 2H, phenyl), 7.82 (d, J = 8.0 Hz, 2H, phenyl), 7.93 (d, J = 8.0 Hz, 4H, phenyl), 8.03 (d, J = 8.0 Hz, 2H, phenyl), 8.26 (d, J = 7.6 Hz, 2H, phenyl), 8.42 (d, J = 8.4 Hz, 2H, phenyl), 8.88 (d, J = 4.4 Hz, 2H, pyrrolic), 8.92 (d, J = 4.4 Hz, 2H, pyrrolic), 8.98 (d, J = 4.8 Hz, 2H, pyrrolic), 9.72 (d, J = 4.8 Hz, 2H, pyrrolic), 9.99 (s, 1H). ^{13}C NMR ($CDCl_3$, 100 MHz,): δ 13.74, 22.03, 28.17, 28.64, 31.24, 38.98, 39.40, 39.82, 54.15, 67.65, 94.00, 95.78, 98.35, 104.84, 109.67, 114.46, 119.96, 122.98, 129.57, 130.88, 134.70, 140.29, 148.34, 150.52, 159.21, 191.23. HRMS (ESI, m/z): $[M + Na]^+$ calcd for $C_{107}H_{131}N_5NaO_5Zn$, 1652.9339; found, 1652.9334.

XW5: A mixture of the porphyrin carboxylate **1s** (90 mg, 0.055 mmol) and $LiOH·H_2O$ (92 mg, 2.2 mmol) in THF (30 mL) and H_2O (2 mL) was refluxed for 12 h under nitrogen. Then, the reaction mixture was diluted with CH_2Cl_2 and washed with H_2O. The organic layer was separated and concentrated in vacuo to afford the crude product, which was purified on a silica gel column to give the product as a red powder (61 mg, yield 68%). ^{1}H NMR ($CDCl_3$:DMSO-d_6 = 1:3, 400 MHz, ppm): 0.31−0.37 (m, 8H), 0.56−0.63 (m, 16H), 0.73−0.78 (m, 20H), 0.86−0.95 (m, 22H), 1.04−1.13 (m, 24H), 1.20−1.27 (m, 2H), 3.83 (t, J = 7.6 Hz, 8H), 7.05 (d, J = 8.0 Hz, 4H, phenyl), 7.38 (t, J = 7.6 Hz, 2H, phenyl), 7.37 (t, J = 7.6 Hz, 2H, phenyl), 7.55 (t, J = 8.4 Hz, 2H, phenyl), 7.68 (t, J = 8.4 Hz, 2H, phenyl), 7.81 (d, J = 8.4 Hz, 2H, phenyl), 7.97 (d, J = 7.6 Hz, 2H, phenyl), 8.25 (d, J = 8.0 Hz, 2H, phenyl), 8.33 (t, J = 8.0 Hz, 4H, phenyl), 8.42 (d, J = 8.0 Hz, 2H, phenyl), 8.66 (d, J = 4.0 Hz, 2H, pyrrolic), 8.72 (d, J = 4.4 Hz, 2H, pyrrolic), 8.77 (d, J = 4.4 Hz, 2H, pyrrolic), 8.87 (d, J = 4.8 Hz, 2H, pyrrolic), 13.08 (s, 1H, COOH). ^{13}C NMR ($CDCl_3$:DMSO-d_6 = 1:2, 100 MHz): δ 13.78, 20.98, 22.02, 24.63, 25.10, 28.10, 28.19, 28.57, 28.63, 28.78, 28.81, 30.30, 31.22, 34.26, 67.00, 104.87, 109.66, 112.97, 117.50, 117.74, 120.01, 120.36, 120.82, 123.00, 124.18, 124.80, 126.00, 127.17, 127.62, 129.51, 129.65, 130.39, 130.68, 131.03, 134.10, 135.48, 136.00, 138.78, 140.29, 142.43, 147.79, 148.22, 148.63, 149.85, 151.41, 159.27, 167.56. HRMS (ESI, m/z): $[M + Na]^+$ calcd for $C_{105}H_{131}N_5NaO_6Zn$, 1644.9289; found, 1644.9283. IR (KBr pellet, cm^{-1}): 3447(br), 2923(s), 2852(s), 1692(m), 1589(m), 1514(w), 1497(w), 1454(s), 1363(w), 1335(w), 1315(w), 1248(m), 1203(w), 1170(w), 1101(s), 999(s), 795(m), 769(w), 748(m), 723(m).

XW6: A mixture of **2s** (90 mg, 0.06 mmol) and cyanoacetic acid (26 mg, 0.30 mmol) in acetonitrile (10 mL) was heated to reflux in the presence of piperidine (1 mL) for 12 h under nitrogen. After cooling, the mixture was diluted with CH_2Cl_2, washed with water, dried over Na_2SO_4, and evaporated in vacuo. The crude product was purified by column chromatography on silica gel to give the product. Yield: 44 mg, 47%. ^{1}H NMR ($CDCl_3$:DMSO-d_6 = 1:3, 400 MHz, ppm): 0.42−0.45 (m, 8H), 0.63−0.64 (m, 16H), 0.74−0.84 (m, 22H), 0.90−0.96 (m, 20H), 1.02−1.14 (m, 26H), 3.83 (t, J = 4.8 Hz, 8H), 7.01 (d, J = 8.8 Hz, 4H, phenyl), 7.34 (t, J = 7.2 Hz, 2H, phenyl), 7.37 (t, J = 7.2 Hz, 2H, phenyl), 7.55 (d, J = 7.6 Hz, 2H, phenyl), 7.65 (t, J = 8.0 Hz, 2H, phenyl), 7.82 (d, J = 8.4 Hz, 2H, phenyl), 7.95 (d, J = 8.0 Hz, 2H, phenyl), 8.27 (d, J = 8.4 Hz, 2H, phenyl), 8.30−8.36 (m, 4H, phenyl), 8.43 (d, J = 8.0 Hz, 2H, phenyl), 8.50 (s, 1H), 8.75−8.78 (m, 4H, pyrrolic), 8.81 (d, J = 4.8 Hz, 2H, pyrrolic), 8.89 (d, J = 4.8 Hz, 2H, pyrrolic). HRMS (ESI, m/z): $[M + Na]^+$ calcd for $C_{108}H_{132}NaN_6O_6Zn$, 1695.9398; found, 1695.9392. IR (KBr pellet, cm^{-1}): 3422(br), 2923(s), 2852(s), 2220(w), 1625(w), 1592(m), 1526(w), 1514(w), 1497(w), 1454(s), 1388(m), 1336(m), 1315(w), 1248(m), 1204(w), 1205(m), 1173(w), 1100(s), 999(s), 811(w), 795(m), 749(m), 723(m).

XW7: It was prepared according to the same procedure as that for **XW6**, except that **3s** (90 mg, 0.06 mmol) was used instead of **2s**. Yield: 36 mg, 38%. ^{1}H NMR ($CDCl_3$:DMSO-d_6 = 1:3, 400 MHz, ppm): 0.41−0.44 (m, 8H), 0.61−0.64 (m, 14H), 0.74−0.81 (m, 22H), 0.92−1.03 (m, 36H), 1.10−1.13 (m, 8H), 1.24−1.27 (m, 4H), 3.88 (t, J = 5. 6 Hz, 8H), 7.06 (d, J = 8.4 Hz, 4H, phenyl), 7.38 (t, J = 7.6 Hz, 2H, phenyl), 7.56 (t, J = 8.0 Hz, 2H, phenyl), 7.71 (t, J = 8.0 Hz, 2H, phenyl), 7.82 (d, J = 8.4 Hz, 2H, phenyl), 7.96 (t, J = 8.0 Hz, 2H, phenyl), 8.10 (d, J = 8.4 Hz, 2H, phenyl), 8.13 (s, 1H), 8.17 (d, J = 7.2 Hz, 2H, phenyl), 8.30 (d, J = 7.6 Hz, 2H, phenyl), 8.40 (d, J = 8.0 Hz, 2H, phenyl), 8.73 (d, J = 4.4 Hz, 2H, pyrrolic), 8.82 (d, J = 4.4 Hz, 4H, pyrrolic), 9.63 (d, J = 4.4 Hz, 2H, pyrrolic). HRMS (ESI, m/z): $[M + Na]^+$ calcd for $C_{110}H_{132}N_6NaO_6Zn$, 1719.9398; found, 1719.9392. IR (KBr pellet, cm^{-1}): 3421(br), 2292(s), 2815(s), 1625(w), 1590(s), 1509(m), 1454(s), 1388(w), 1363(w), 1335(w), 1315(w), 1248(m),

DOI: 10.1021/acsami.5b06610
ACS Appl. Mater. Interfaces 2015, 7, 21956−21965

1230(m), 1206(w), 1185(w), 1000(s), 998(s), 946(w), 837(w), 811(w), 795(m), 770(w), 748(m), 723(m).

XW8: It was prepared with reference to the procedure reported by Grätzel and co-workers.[55] A mixture of porphyrin **5** (150 mg, 0.095 mmol), **4** (122 mg, 0.474 mmol), $Pd(PPh_3)_4$ (23 mg, 0.020 mmol), CuI (4 mg, 0.02 mmol), and K_2CO_3 (29 mg, 0.21 mmol) was put into a 100 mL Schlenk flask. Later on, piperidine (0.235, 2.74 mmol), THF (30 mL), and methanol (5 mL) were added into the flask, and the reaction mixture was refluxed for 48 h under nitrogen. Then the mixture was diluted with H_2O and CH_2Cl_2. The organic layer was separated and subsequently dried over anhydrous Na_2SO_4. The solvent was removed, and the residue was purified on a silica gel column to obtain **XW8** as a dark green solid, which was further purified by recrystallization in CH_2Cl_2 and MeOH. Yield: 39 mg, 18%. ^1H NMR ($CDCl_3$:DMSO-d_6 = 1:3, 400 MHz, ppm): 0.32−0.35 (m, 8H), 0.44−0.59 (m, 16H), 0.72−0.78 (m, 20H), 0.86−1.00 (m, 40H), 1.07−1.12 (m, 8H), 3.87 (t, J = 5.6 Hz, 8H), 7.10 (d, J = 8.4 Hz, 4H, phenyl), 7.39 (t, J = 7.2 Hz, 2H, phenyl), 7.56 (t, J = 8.0 Hz, 2H, phenyl), 7.73 (t, J = 8.4 Hz, 2H, phenyl), 7.81 (d, J = 8.0 Hz, 2H, phenyl), 7.98 (d, J = 8.0 Hz, 2H, phenyl), 8.29 (d, J = 7.6 Hz, 2H, phenyl), 8.39 (d, J = 8.0 Hz, 2H, phenyl), 8.47 (s, 1H, phenyl), 8.70 (d, J = 4.8 Hz, 2H, pyrrolic), 8.78 (d, J = 4.4 Hz, 2H, pyrrolic), 8.81 (d, J = 4.4 Hz, 2H, pyrrolic), 9.66 (d, J = 4.4 Hz, 2H, pyrrolic). HRMS (ESI, m/z): $[M + Na]^+$ calcd for $C_{108}H_{130}N_6NaO_6Zn$, 1693.9241; found, 1693.9235. IR (KBr pellet, cm^{-1}): 3446(br), 2923(s), 2852(s), 2185(m), 1695(m), 1593(s), 1525(w), 1507(w), 1455(s), 1379(w), 1336(w), 1249(m), 1207(w), 1101(s), 999(s), 794(m), 749(m), 724(m).

Theoretical Approach. Density functional theory (DFT) calculations using the hybrid B3LYP functional[61,62] and the 6-31G* basis set[63] were employed to optimize the ground state geometries of compounds **XW5**−**XW8**. All calculations were performed using the Gaussian09 program package.[64] The Los Alamos effective core potential basis set (LANL2DZ) is used for the zinc atom.[65] Time-dependent DFT calculations were carried out at the optimized geometries using the M06 density functional.[66]

Photovoltaic Device Fabrication. The procedure reported by Grätzel and co-workers[67] was adapted to prepare the TiO_2 electrodes and fabricate the sealed cells for photovoltaic measurements. The TiO_2 films which were obtained by a screen-printing method with a working area of 0.12 cm^2 were used as the photoelectrode. First, a 12 μm thick film of 13 nm sized TiO_2 particles was printed on the FTO glass. Later on, the FTO glass coated with TiO_2 film was kept in a clean box for 5 min, dried at 125 °C for 6 min, and then coated with a 5 μm thick second layer of 400 nm light-scattering anatase particles. Finally, the electrodes were gradually sintered in a muffle furnace at 275 °C for 5 min, at 325 °C for 5 min, at 375 °C for 5 min, at 450 °C for 15 min, and at 500 °C for 15 min, respectively. Before use, these films were immersed into a 40 mM aqueous $TiCl_4$ solution at 70 °C for 30 min, washed with water and ethanol, and then heated again at 450 °C for 30 min, after which the films were immersed into a 0.2 mM solution of the porphyrin dyes **XW5**−**XW8** and **XW1** in a mixture of toluene and ethanol (volume ratio of 1:4) at room temperature for 10 h. As for cosensitization,[68] these porphyrin-sensitized films were washed with ethanol, dried in air, and immersed in a solution of **XS3** (0.3 mM) in a mixture of chloroform and ethanol (volume ratio of 3:7) at room temperature for 1 h. For preparing the Pt counter electrode, the FTO glass was sputtered with three drops of 0.02 M H_2PtCl_6 in 2-propanol and followed by annealing treatment at 400 °C for 15 min subsequently, and a hole (diameter of 0.8 mm) was drilled on the counter electrode. The perforated sheet was cleaned by ultrasound in ethanol for 10 min. To fabricate the DSSC devices, the dye-covered TiO_2 electrode and Pt-counter electrode were tightly clipped together into a sandwich-type cell and sealed with a hot-melt gasket of 25 μm thickness made of ionomer Sulyn 1702 (DuPont). The electrolyte solution L130, which consists of 0.1 M LiI, 0.05 M I2, 0.6 M 1-methyl-3-propyl-imidazolium iodide (PMII), and 0.5 M 4-*tert*-butylpyridine (TBP) in a mixture of acetonitrile and valeronitrile (volume ratio of 85:15), was introduced into the cell through the hole in the back of the counter electrode. Then the hole was sealed by a UV-melt gum and a cover glass.

Electrochemistry and Photoelectrochemistry. Cyclic voltammetry measurements were conducted in acetonitrile with a scan rate of 100 mV s^{-1} using a Versastat II electrochemical workstation (Princeton Applied Research), which used 0.1 M $TBAPF_6$ (Aldrich) as the supporting electrolyte, the sensitizer attached to a nanocrystalline TiO_2 film deposited on the conducting FTO glass as the working electrode, a platinum wire as the counter electrode, and a regular calomel electrode in saturated KCl solution as the reference electrode. Photovoltaic properties were measured by employing an AM 1.5 solar simulator equipped with a 300 W xenon lamp (model no. 91160, Oriel). The incident light intensity was calibrated to 100 mW cm^{-2} with a Newport Oriel PV reference cell system (model 91150 V), and the J−V curves were obtained by applying an external bias to the cell and measuring the generated photocurrent with a model 2400 source meter (Keithley Instruments, Inc. USA). The voltage step and delay time of the photocurrent were 10 mV and 40 ms, respectively. The incident monochromatic photon-to-electron conversion efficiency (IPCE) of the solar cells was recorded using a Newport-74125 system (Newport Instruments), and the intensity of monochromatic light was measured with a Si detector (Newport-71640). The electrochemical impedance spectroscopy (EIS) measurements were achieved on a Zahner IM6e Impedance Analyzer (ZAHNER-Elektrik GmbH & CoKG, Kronach, Germany), of which the frequency ranged between 0.1 Hz and 100 kHz, and the alternative signal was 10 mV. The data were later plotted with ZSimp-Win software.

Stability Study. For photostability study, the absorbance of the dyes adsorbed on the nanocrystalline films was evaluated for four times after irradiation for 0, 5, 15, and 30 min, respectively. The irradiation was performed by visible light (>420 nm) from a solar simulator operating at AM 1.5 (100 mW cm^{-2}) with an ultraviolet cutoff filter.

■ ASSOCIATED CONTENT

Ⓢ Supporting Information

The Supporting Information is available free of charge on the ACS Publications website at DOI: 10.1021/acsami.5b06610.

Characterization data for the compounds and additional figures (PDF)

■ AUTHOR INFORMATION

Corresponding Authors

*E-mail: yshxie@ecust.edu.cn.
*E-mail: lixin@theochem.kth.se.

Notes

The authors declare no competing financial interest.

■ ACKNOWLEDGMENTS

This work was supported by the Science Fund for Creative Research Groups (21421004), NSFC/China (21472047, 91227201), and the Oriental Scholarship. X.L. and H.Å. acknowledge computational resources provided by the Swedish National Infrastructure for Computing (SNIC 2014/11-31).

■ REFERENCES

(1) O'Regan, B.; Grätzel, M. A Low-Cost, High-Efficiency Solar Cell Based on Dye-Sensitized Colloidal TiO_2 Films. *Nature* **1991**, *353*, 737−740.

(2) Grätzel, M. Photoelectrochemical Cells. *Nature* **2001**, *414*, 338−344.

(3) Hamann, T. W.; Ondersma, J. W. Dye-sensitized Solar Cell Redox Shuttles. *Energy Environ. Sci.* **2011**, *4*, 370−381.

(4) Wu, K. L.; Ho, S. T.; Chou, C. C.; Chang, Y. C.; Pan, H. A.; Chi, Y.; Chou, P. T. Engineering of Osmium(II)-Based Light Absorbers for Dye-Sensitized Solar Cells. *Angew. Chem., Int. Ed.* **2012**, *51*, 5642−5646.

DOI: 10.1021/acsami.5b06610
ACS Appl. Mater. Interfaces 2015, 7, 21956−21965

(5) Jiang, S.; Lu, X.; Zhou, G.; Wang, Z. S. Charge Transfer in Cross Conjugated 4, 8-Dithienylbenzo [1, 2-b:4, 5-b′] Dithiophene Based Organic Sensitizers. *Chem. Commun.* **2013**, *49*, 3899−3901.
(6) Feng, Q.; Jia, X.; Zhou, G.; Wang, Z. S. Embedding an Electron Donor or Acceptor into Naphtho[2,1-b:3,4-b′] Dithiophene Based Organic Sensitizers for Dye-Sensitized Solar Cells. *Chem. Commun.* **2013**, *49*, 7445−7447.
(7) Zhang, S. F.; Yang, X. D.; Numata, Y.; Han, L. Y. Highly Efficient Dye-Sensitized Solar Cells: Progress and Future Challenges. *Energy Environ. Sci.* **2013**, *6*, 1443−1464.
(8) Grätzel, M.; Janssen, R. A. J.; Mitzi, D. B.; Sargent, E. H. Materials Interface Engineering for Solution-Processed Photovoltaics. *Nature* **2012**, *488*, 304−312.
(9) Wu, Y. Z.; Zhu, W. H. Organic Sensitizers from D-π-A to D-A-π-A: Effect of the Internal Electron-withdrawing Units on Molecular Absorption, Energy Levels and Photovoltaic Performances. *Chem. Soc. Rev.* **2013**, *42*, 2039−2058.
(10) Urbani, M.; Grätzel, M.; Nazeeruddin, M. K.; Torres, T. Meso-Substituted Porphyrins for Dye-Sensitized Solar Cells. *Chem. Rev.* **2014**, *114*, 12330−12396.
(11) Chou, C. C.; Hu, F. C.; Yeh, H. H.; Wu, H. P.; Chi, Y.; Clifford, J. N.; Palomares, E.; Liu, S. H.; Chou, P. T.; Lee, G. H. Highly Efficient Dye-Sensitized Solar Cells Based on Pan-chromatic Ruthenium Sensitizers with Quinolinylbipyridine Anchors. *Angew. Chem., Int. Ed.* **2014**, *53*, 178−183.
(12) Zhang, S. F.; Yang, X. D.; Qin, C. J.; Numata, Y.; Han, L. Y. Interfacial Engineering for Dye-Sensitized Solar Cells. *J. Mater. Chem. A* **2014**, *2*, 5167−5177.
(13) Liu, J.; Numata; Qin, C. J.; Islam, A.; Yang, X. D.; Han, L. Y. Circle Chain Embracing Donor-acceptor Organic Dye: Simultaneous Improvement of Photocurrent and Photovoltage for Dye-Sensitized Solar Cells. *Chem. Commun.* **2013**, *49*, 7587−7589.
(14) Ren, X. M.; Jiang, S. H.; Cha, M. Y.; Zhou, G.; Wang, Z. S. Thiophene-Bridged Double D-π-A dye for Efficient Dye-Sensitized Solar Cell. *Chem. Mater.* **2012**, *24*, 3493−3499.
(15) Das, S. K.; Song, B. Y.; Mahler, A.; Nesterov, V. N.; Wilson, A. K.; Ito, O.; D'Souza, F. Electron Transfer Studies of High Potential Zinc Porphyrin-Fullerene Supramolecular Dyads. *J. Phys. Chem. C* **2014**, *118*, 3994−4006.
(16) Ding, Y. B.; Tang, Y. Y.; Zhu, W. H.; Xie, Y. S. Fluorescent and Colorimetric Ion Probes Based on Conjugated Oligopyrroles. *Chem. Soc. Rev.* **2015**, *44*, 1101−1112.
(17) Xie, Y. S.; Yamaguchi, K.; Toganoh, M.; Uno, H.; Suzuki, M.; Mori, S.; Saito, S.; Osuka, A.; Furuta, H. Triply N-confused Hexaphyrins: Near-Infrared Luminescent Dyes with aTriangular Shape. *Angew. Chem., Int. Ed.* **2009**, *48*, 5496−5499.
(18) Xie, Y. S.; Wei, P. C.; Li, X.; Hong, T.; Zhang, K.; Furuta, H. Macrocycle Contraction and Expansion of a Dihydrosapphyrin Isomer. *J. Am. Chem. Soc.* **2013**, *135*, 19119−10122.
(19) Wei, P. C.; Zhang, K.; Li, X.; Meng, D. Y.; Ågren, H.; Ou, Z.; Ng, S.; Furuta, H.; Xie, Y. S. Neo-Fused Hexaphyrin: A Molecular Puzzle Containing an N-Linked Pentaphyrin. *Angew. Chem., Int. Ed.* **2014**, *53*, 14069−14073.
(20) Zhang, K.; Wei, P. C.; Li, X.; Ågren, H.; Xie, Y. S. Oxi-dative Ring Closure and Metal Triggered Ring Opening: Syntheses of Macrocyclic and Linear Hexapyrroles. *Org. Lett.* **2014**, *16*, 6354−6357.
(21) Xie, Y. S.; Hill, J. P.; Charvet, R.; Ariga, K. J. Porphyrin Colorimetric Indicators in Molecular and Nano-Architectures. *J. Nanosci. Nanotechnol.* **2007**, *7*, 2969−2993.
(22) D'Souza, F. Expanded Porphyrins: More Confusion All the Time. *Angew. Chem., Int. Ed.* **2015**, *54*, 4713−4714.
(23) Li, Z.; Li, Q. Q. Molecular Engineering and Cosensitization for Developing Efficient Solar Cells Based on Porphyrin Dyes with an Extended Framework. *Sci. China: Chem.* **2014**, *57*, 1491−1491.
(24) Hsieh, C. P.; Lu, H. P.; Chiu, C. L.; Lee, C. W.; Chuang, S. H.; Mai, C. L.; Yen, W. N.; Hsu, S. J.; Diau, E. W.G.; Yeh, C. Y. Synthesis and Characterization of Porphyrin Sensitizers with Various Electron-Donating Substituents for Highly Efficient Dye-Sensitized Solar Cells. *J. Mater. Chem.* **2010**, *20*, 1127−1134.
(25) Pellejá, L.; Kumar, C. V.; Clifford, J. N.; Palomares, E. D-π-A Porphyrin Employing an Indoline Donor Group for High Efficiency Dye-Sensitized Solar Cells. *J. Phys. Chem. C* **2014**, *118*, 16504−16509.
(26) Lee, C. W.; Lu, H. P.; Lan, C. M.; Huang, Y. L.; Liang, Y. R.; Yen, W. N.; Liu, Y. C.; Lin, Y. S.; Diau, E. W. G.; Yeh, C. Y. Novel Zinc Porphyrin Sensitizers for Dye-Sensitized Solar cells: Synthesis and Spectral, Electrochemical, and Photovoltaic Properties. *Chem. - Eur. J.* **2009**, *15*, 1403−1412.
(27) Wu, S. L.; Lu, H. P.; Yu, H. T.; Chuang, S. H.; Chiu, C. L.; Lee, C. W.; Diau, E. W. G.; Yeh, C.-Y. Design and Characterization of Porphyrin Sensitizers with a Push-Pull Framework for Highly Efficient Dye-Sensitized Solar Cells. *Energy Environ. Sci.* **2010**, *3*, 949−955.
(28) Bessho, T.; Zakeeruddin, S. M.; Yeh, C. Y.; Diau, E. W.G.; Grätzel, M. Highly Efficient Mesoscopic Dye-Sensitized Solar Cells Based on Donor-Acceptor-Substituted Porphyrins. *Angew. Chem., Int. Ed.* **2010**, *49*, 6646−6649.
(29) Mathew, S.; Iijima, H.; Toude, Y.; Umeyama, T.; Matano, Y.; Ito, S.; Tkachenko, N. V.; Lemmetyinen, H.; Imahori, H. Optical, Electrochemical, and Photovoltaic Effects of an Electron-Withdrawing Tetrafluorophenylene Bridge in a Push-Pull Porphyrin Sensitizer Used for Dye-Sensitized Solar Cells. *J. Phys. Chem. C* **2011**, *115*, 14415−14424.
(30) Liu, B.; Zhu, W. H.; Wang, Y. Q.; Wu, W. J.; Li, X.; Chen, B. Q.; Long, Y. T.; Xie, Y. S. Modulation of Energy Levels by Donor Groups: an Effective Approach for Optimizing the Efficiency of Zinc-Porphyrin Based Solar Cells. *J. Mater. Chem.* **2012**, *22*, 7434−7444.
(31) Mathew, S.; Yella, A.; Gao, P.; Humphry-Baker, R.; Cur-chod, B. F. E.; Ashari-Astani, N.; Tavernelli, I.; Rothlisberger, U.; Nazeeruddin, M. K.; Grätzel, M. Dye-Sensitized Solar Cells with 13% Efficiency Achieved Through the Molecular Engineering of Porphyrin Sensitizers. *Nat. Chem.* **2014**, *6*, 242−247.
(32) Gabrielsson, E.; Tian, H. N.; Eriksson, S. K.; Gao, J. J.; Chen, H.; Li, F. S.; Oscarsson, J.; Sun, J. L.; Rensmo, H.; Kloo, l.; Hagfeldt, A.; Sun, L. C. Dipicolinic Acid: a Strong Anchoring Group with Tunable Redox and Spectral Behavior for Stable Dye-Sensitized Solar Cells. *Chem. Commun.* **2015**, *51*, 3858−3861.
(33) Lu, J. F.; Xu, X. B.; Cao, K.; Cui, J.; Zhang, Y. B.; Shen, Y.; Shi, X. B.; Liao, L. S.; Cheng, T. B.; Wang, M. K. D-π-A Structured Porphyrins for Efficient Dye-Sensitized Solar Cells. *J. Mater. Chem. A* **2013**, *1*, 10008−10015.
(34) Wang, Y. Q.; Xu, L.; Wei, X. D.; Li, X.; Ågren, H.; Wu, W. J.; Xie, Y. S. 2-Diphenylaminothiophene as the Donor of Porphyrin Sensitizers for Dye-Sensitized Solar Cells. *New J. Chem.* **2014**, *38*, 3227−3235.
(35) Ladomenou, k.; Kitsopoulos, T. N.; Sharma, G. D.; Coutsolelos, A. G. The Importance of Various Anchoring Groups Attached on Porphyrins as Potential Dyes for DSSC Applications. *RSC Adv.* **2014**, *4*, 21379−21404.
(36) Liu, Y. Z.; Lin, H.; Dy, J.; Tamaki, K.; Nakazaki, J.; Naka-yama, D.; Uchida, S.; Kubo, T.; Segawa, H. N-Fused Carbazole−Zinc Porphyrin-Free-Base Porphyrin Triad for Efficient Near-IR Dye-Sensitized Solar Cells. *Chem. Commun.* **2011**, *47*, 4010−4012.
(37) Wang, Y. Q.; Chen, B.; Wu, W. J.; Li, X.; Zhu, W. H.; Tian, H.; Xie, Y. S. Efficient Solar Cells Sensitized by Porphyrins with an Extended Conjugation Framework and a Carbazole Donor: From Molecular Design to Cosensitization. *Angew. Chem., Int. Ed.* **2014**, *53*, 10779−10783.
(38) Wang, Y. Q.; Li, X.; Liu, B.; Wu, W. J.; Zhu, W. H.; Xie, Y. S. Porphyrins Bearing Long Alkoxyl Chains and Carbazole for Dye-Sensitized Solar Cells: Tuning Cell Performance Through an Ethynylene Bridge. *RSC Adv.* **2013**, *3*, 14780−14790.
(39) Chitpakdee, C.; Namuangruk, S.; Suttisintong, K.; Jung-suttiwong, S.; Keawin, T.; Sudyoadsuk, T.; Sirithip, K.; Promarak, V.; Kungwan, N. Effects of π-linker, Anchoring Group and Capped Carbazole at Meso-Substituted Zinc-Porphyrins on Conversion Efficiency of DSSCs. *Dyes Pigm.* **2015**, *118*, 64−75.
(40) Ripolles-Sanchis, T.; Guo, B. C.; Wu, H. P.; Pan, T. Y.; Lee, H. W.; Raga, S. R.; Fabregat-Santiago, F.; Bisquert, J.; Yeh, C. Y.; Diau, E. W. G. Design and Characterization of Alkoxy-Wrapped Push-Pull

DOI: 10.1021/acsami.5b06610
ACS Appl. Mater. Interfaces 2015, 7, 21956−21965

Porphyrins for Dye-Sensitized Solar Cells. *Chem. Commun.* **2012**, *48*, 4368−4370.
(41) Li, W. H.; Liu, Z. H.; Wu, W. H.; Cheng, Y. B.; Zhao, Z. X.; He, H. S. Thiophene-Functionalized Porphyrins: Synthesis, Photophysical Properties, and Photovoltaic Performance in Dye-Sensitized Solar Cells. *J. Phys. Chem. C* **2015**, *119*, 5265−5273.
(42) Chang, Y. C.; Wu, H. P.; Reddy, N. M.; Lee, H. W.; Lu, H. P.; Yeh, C. Y.; Diau, E. W. G. The Influence of Electron Injection and Charge Recombination Kinetics on the Performance of Porphyrin-Sensitized Solar Cells: Effects of the 4-Tert-Butylpyridine Additive. *Phys. Chem. Chem. Phys.* **2013**, *15*, 4651−4655.
(43) Jradi, F. M.; Kang, X. W.; O'Neil, D.; Pajares, G.; Get-manenko, Y. A.; Szymanski, P.; Parker, T. C.; ElSayed, M. A.; Marder, S. R. Near-Infrared Asymmetrical Squaraine Sensitizers for Highly Efficient Dye Sensitized Solar Cells: The Effect of π-Bridges and Anchoring Groups on Solar Cell Performance. *Chem. Mater.* **2015**, *27*, 2480−2487.
(44) Zhou, N. J.; Prabakaran, K.; Lee, B. H.; Chang, S. H.; Harutyunyan, K.; Guo, P. J.; Butler, M. R.; Timalsina, A.; Bedzyk, M. J.; Ratner, M. A.; Vegiraju, S.; Yau, S.; Wu, C. G.; Chang, R. P. H.; Facchetti, A.; Chen, M. C.; Marks, T. B. Metal-Free Tetrathienoacene Sensitizers for High-Performance Dye-Sensitized Solar Cells. *J. Am. Chem. Soc.* **2015**, *137*, 4414−4423.
(45) Chen, Y. F.; Liu, J. M.; Huang, J. F.; Tan, L. L.; Shen, Y.; Xiao, L. M.; Kuang, D. B.; Su, C. Y. Stable Organic dyes Based on the Benzo[1,2-b:4,5-b′]-Dithiophene Donor for Efficient Dye-Sensitized Solar Cells. *J. Mater. Chem. A* **2015**, *3*, 8083−8090.
(46) Sun, X.; Wang, Y. Q.; Li, X.; Ågren, H.; Zhu, W. H.; Tian, H.; Xie, Y. S. Cosensitizers for Simultaneous Filling Up of Both Absorption Valleys of Porphyrins: A Novel Approach for Developing Efficient Panchromatic Dye-Sensitized Solar Cells. *Chem. Commun.* **2014**, *50*, 15609−15612.
(47) Hagfeldt, A.; Boschloo, G.; Sun, L.; Kloo, L.; Pettersson, H. Dye-Sensitized Solar Cells. *Chem. Rev.* **2010**, *110*, 6595−6653.
(48) Giribabu, L.; Kanaparthi, R. K.; Velkannan, V. Molecular Engineering of Sensitizers for Dye-Sensitized Solar Cell Applications. *Chem. Rec.* **2012**, *12*, 306−328.
(49) Kim, B. G.; Chung, K.; Kim, J. Molecular Design Principle of All-organic Dyes for Dye-Sensitized Solar Cells. *Chem. - Eur. J.* **2013**, *19*, 5220−5230.
(50) Clifford, J. N.; Martinez-Ferrero, E.; Viterisi, A.; Palomares, E. Sensitizer Molecular Structure-Device Efficiency Relationship in Dye Sensitized Solar Cells. *Chem. Soc. Rev.* **2011**, *40*, 1635−1646.
(51) Kang, M. S.; Kang, S. H.; Kim, S. G.; Choi, I. T.; Ryu, J. H.; Ju, M. J.; Cho, F.; Lee, J. Y.; Kim, H. K. Novel D-π-A Structured Zn(II)-Porphyrin Dyes Containing a Bis(3,3-dimethylfluorenyl)Amine Moiety for Dye-Sensitized Solar Cells. *Chem. Commun.* **2012**, *48*, 9349−9351.
(52) Shi, J.; Chai, Z. F.; Tang, R. L.; Hua, J. L.; Li, Q. Q.; Li, Z. New Triphenylamine-Based Sensitizers Bearing Double Anchoring Units for Dye-Sensitized Solar Cells. *Sci. China: Chem.* **2015**, *58*, 1144−1151.
(53) Zeng, J.; Zhang, T. L.; Zang, X. F.; Kuang, D. B.; Meier, H.; Cao, D. R. D-A-π-A Organic Sensitizers Containing a Benzothiazole Moiety as an Additional Acceptor for Use in Solar Cells. *Sci. China: Chem.* **2013**, *56*, 505−513.
(54) Chai, Z. F.; Wu, M.; Fang, M. M.; Wan, S. S.; Xu, T.; Tang, R. L.; Xie, Y. J.; Mei, A. Y.; Han, H. W.; Li, Q. Q.; Li, Z. Similar or Totally Different: the Adjustment of the Twist Conformation Through Minor Structural Modification, and Dramatically Improved Performance for Dye-Sensitized Solar Cell. *Adv. Energy Mater.* **2015**.
(55) Hagberg, D. P.; Yum, J.; Lee, H. H.; De Angelis, F.; Mari-nado, T.; Karlsson, K. M.; Baker, R. H.; Sun, L. C.; Hagfeldt, A.; Grätzel, M.; Nazeeruddin, M. K. Molecular Engineering of Organic Sensitizers for Dye-Sensitized Solar Cell Applications. *J. Am. Chem. Soc.* **2008**, *130*, 6259−6266.
(56) Yan, C. C.; Ma, W. T.; Ren, Y. M.; Zhang, M.; Wang, P. Efficient Triarylamine−Perylene Dye-Sensitized Solar Cells: Influence of Triple-Bond Insertion on Charge Recombination. *ACS Appl. Mater. Interfaces* **2015**, *7*, 801−809.
(57) Yella, A.; Lee, H. W.; Tsao, H. N.; Yi, C. Y.; Chandiran, A. K.; Nazeeruddin, M. K.; Diau, E.W. G.; Yeh, C. Y.; Zakeeruddin, S. M.; Grätzel, M. Porphyrin-Sensitized Solar Cells with Cobalt (II/III)-Based Redox Electrolyte Exceed 12% Efficiency. *Science* **2011**, *334*, 629−634.
(58) Shi, Y. B.; Liang, M.; Wang, L.; Han, H. Y.; You, L. S.; Sun, Z.; Xue, S. New Ruthenium Sensitizers Featuring Bulky Ancil-lary Ligands Combined with a Dual Functioned Coadsorbent for High Efficiency Dye-Sensitized Solar Cells. *ACS Appl. Mater. Interfaces* **2013**, *5*, 144−153.
(59) Katono, M.; Bessho, T.; Wielopolski, M.; Marszalek, M.; Moser, J. E.; Humphry-Baker, R.; Zakeeruddin, S. M.; Grätzel, M. *J. Phys. Chem. C* **2012**, *116*, 16876−16884.
(60) Katono, M.; Bessho, T.; Meng, S.; Humphry-Baker, R.; Rothenberger, G.; Zakeeruddin, S. M.; Kaxiras, E.; Grätzel, M. D-π-A Dye System Containing Cyano-Benzoic Acid as Anchoring Group for Dye-Sensitized Solar Cells. *Langmuir* **2011**, *27*, 14248−14252.
(61) Becke, A. D. Density-Functional Thermochemistry. III. The role of exact exchange. *J. Chem. Phys.* **1993**, *98*, 5648−5652.
(62) Lee, C.; Yang, W. T.; Parr, R. G. Development of the Colle-Salvetti Correlation-Energy Formula into a Functional of the Electron Density. *Phys. Rev. B: Condens. Matter Mater. Phys.* **1988**, *37*, 785−789.
(63) Hehre, W. J.; Ditchfield, R.; Pople, J. A. Self-Consistent Molecular Orbital Methods. XII. Further Extensions of Gaussian-Type Basis Sets for Use in Molecular Orbital Studies of Organic Molecules. *J. Chem. Phys.* **1972**, *56*, 2257−2261.
(64) Frisch, M. J.; Trucks, G. W.; Schlegel, H. B.; Scuseria, G. E.; Robb, M. A.; Cheeseman, J. R.; Scalmani, G.; Barone, V.; Mennucci, B.; Petersson, G. A.; Nakatsuji, H.; Caricato, M.; Li, X.; Hratchian, H. P.; Izmaylov, A. F.; Bloino, J.; Zheng, G.; Sonnenberg, J. L.; Hada, M.; Ehara, M.; Toyota, K.; Fukuda, R.; Hasegawa, J.; Ishida, M.; Nakajima, T.; Honda, Y.; Kitao, O.; Nakai, H.; Vreven, T.; Montgomery, J. A., Jr.; Peralta, J. E.; Ogliaro, F.; Bearpark, M.; Heyd, J. J.; Brothers, E.; Kudin, K. N.; Staroverov, V. N.; Kobayashi, R.; Normand, J.; Raghavachari, K.; Rendell, A.; Burant, J. C.; Iyengar, S. S.; Tomasi, J.; Cossi, M.; Rega, N.; Millam, J. M.; Klene, M.; Knox, J. E.; Cross, J. B.; Bakken, V.; Adamo, C.; Jaramillo, J.; Gomperts, R.; Stratmann, R. E.; Yazyev, O.; Austin, A. J.; Cammi, R.; Pomelli, C.; Ochterski, J. W.; Martin, R. L.; Morokuma, K.; Zakrzewski, V. G.; Voth, G. A.; Salvador, P.; Dannenberg, J. J.; Dapprich, S.; Daniels, A. D.; Farkas, Ö.; Foresman, J. B.; Ortiz, J. V.; Cioslowski, J.; Fox, D. J. *Gaussian 09*, revision D.01; Gaussian, Inc.: Wallingford, CT, 2009.
(65) Hay, P. J.; Wadt, W. R. Abinitio Effective Core Potentials for Molecular Calculations. Potentials for the Transition Metal Atoms Scandium to Mercury. *J. Chem. Phys.* **1985**, *82*, 270−283.
(66) Zhao, Y.; Truhlar, D. G. The M06 Suite of Density Functionals for Main Group Thermochemistry, Thermochemistry Kinetics, Noncovalent Interactions, Excited States, and Transition Elements: Two New Functionals and Systematic Testing of Four M06-Class Funvtionals and 12 Other Functionals. *Theor. Chem. Acc.* **2008**, *120*, 215−241.
(67) Ito, S.; Murakami, T. N.; Comte, P.; Liska, P.; Grätzel, C.; Nazeeruddin, M. K.; Grätzel, M. Fabrication of Thin Film Dye Sensitized Solar Cells with Solar to Electric Power Conversion Efficiency Over 10%. *Thin Solid Films* **2008**, *516*, 4613−4619.
(68) Lan, C. M.; Wu, H. P.; Pan, T. Y.; Chang, C. W.; Chao, W. S.; Chen, C. T.; Wang, C. L.; Lin, C. Y.; Diau, E. W. G. Enhanced Photovoltaic Performance with Co-Sensitization of Porphyrin and an Organic Dye in Dye-Sensitized Solar Cells. *Energy Environ. Sci.* **2012**, *5*, 6460−6464.

DOI: 10.1021/acsami.5b06610
ACS Appl. Mater. Interfaces 2015, 7, 21956−21965